Raizada et al. Earth, Planets and Space (2015) 67:146
DOI 10.1186/s40623-015-0322-z

Earth, Planets and Space
a SpringerOpen Journal

FULL PAPER Open Access

Dependence of mesospheric Na and Fe distributions on electron density at Arecibo

Shikha Raizada[1*], Craig A. Tepley[1], Qihou Zhou[2], Sumanta Sarkhel[3], John D. Mathews[4], Nestor A. Aponte[1], Ilgin Seker[5], Robert Kerr[1] and Edvier Cabassa[1]

Abstract

We present case studies of the mesospheric alkali and non-alkali metals, Na and Fe, along with electron concentrations [N_e] obtained from measurements made at Arecibo on nights of 17–18 and 18–19 March 2004. The background mesospheric conditions as recorded by an airglow all-sky imager displayed ripple- and band-type structures on these nights. Both of the metals display detailed structures within their neutral sporadic layer but are more pronounced in Na than for Fe. A sporadic-E (E_s) with electron concentrations [N_e] exceeding 3000 electrons cm^{-3} is accompanied by a strong Na enhancement and a weak sporadic Fe (Fe_s) layer around 95-km altitude. The concentration of Fe^+ and Na^+ is estimated to be close to 600 and 30 ions.cm^{-3}, respectively, within the sporadic-E layer. In order to investigate ion-neutral coupling, a correlative analysis was performed in two altitude regions. Similar features are seen between neutrals and electrons in the 96–100-km altitude range, while within the altitude range of 80–90 km, an opposite behavior is seen. A comparative study between neutral layers below 90 km often referred to as the main or permanent layer and sporadic activity above 90 km reveals different characteristics for alkali and non-alkali metal. Fe concentrations in the main layer are higher than in Fe_s resulting in a density ratio of less than 1 determined from two layers of 3 km thickness centered at 97 and 87 km. For the case of Na, the ratio exceeds 1 during E_s activity on both the nights.
The case studies discussed in this work facilitate our understanding of different factors that can influence the sporadic activity in alkali and non-alkali metals. In a region dominated by ion-molecule chemistry, temperature fluctuations that can be induced by wave activity will have more impact on Na than for Fe within their layers depending on altitude.

Keywords: Mesospheric layers; Sporadic-E; Ion-neutral coupling; ISR

Background

A variety of interesting phenomena occur in the mesospheric region of the Earth's atmosphere that includes sporadic-E (Whitehead, 1989), polar mesospheric summer echoes (Rapp and Lübken, 2004), and deposition of meteoric metals (Gadsden, 1969; Plane, 2003). The existence of metals in the Earth's mesosphere was first established using airglow studies (Brown, 1973). With the advent of laser technology, several groups reported temporal and altitudinal distributions of various metals like Na, K, Ca, and Fe using ground-based lidar systems located at different latitudes (Alpers et al., 1990,1994; Tepley et al., 2003; Collins et al., 1994; Clemesha et al., 2004; Sridharan et al., 2009; Gardner et al., 2011; Raizada et al., 2011; Yuan et al., 2012). This led to the development of modeling efforts to understand mesospheric chemistry and the role of meteor input in the distribution of metals (Plane, 2003). One of the most abundant metals in meteoroids as well as in the mesosphere is atomic Fe. Upper atmospheric atomic Fe has been studied from different locations (Granier et al. 1989, Alpers et al., 1990; Kane and Gardner, 1993; Chu et al., 2006; Raizada and Tepley, 2002, Huang et al., 2013). Raizada and Tepley (2003) found significant latitudinal differences in the Fe distribution. Observations of Fe at South Pole and Rothera have shown seasonal differences in its distribution (Gardner et al., 2011). In addition to the main or permanent metal layer, earlier studies have shown the occurrence of thin regions of enhanced concentrations occasionally, generally referred to as sporadic layers in the neutrals. A strong link between these sporadic layers and sporadic-E has been suggested in many earlier studies (Kirkwood and von Zahn, 1991; Gardner et al., 1993;

* Correspondence: Shikha@naic.edu
[1]Space and Atmospheric Sciences, Arecibo Observatory, SRI International, Arecibo, PR, USA
Full list of author information is available at the end of the article

Alpers et al., 1994; Collins et al., 2002; Williams et al., 2007; Zhou et al., 2008). Sporadic-E is often patchy in nature, i.e., the electron concentrations display spatial variations and hence result in inhomogeneity in the atmosphere (Miller and Smith, 1975). Observations of Fe by Alpers et al. (1990) from Andoya, Norway (69° N) revealed frequent occurrences of Fe_s within 15 h. A more comprehensive comparison of Na and Fe layers at mid-latitudes showed sporadic activity to be very prominent for Fe but not so for Na (Kane and Gardner, 1993). The latitudinal variation in the occurrence of Na_s layers is evident from the following studies: Nagasawa and Abo (1995) reported frequent observations of sporadic Na layers above Tokyo (35.6° N). Yi et al. (2002) studied the seasonal variability of Na_s layers over Wuhan (30.5° N), China and found that their occurrence rate maximized in summer. Their study revealed broader Na_s widths as compared to low and high latitudes. Recent work by Wang et al. (2012) have shown that at 40° N double layers in Na occurred between 105 and 130 km with about 17 such events per 319 of total observations. Later on, Dou et al. (2013) analyzed Na lidar data from four sites (40° N, 31° N, 30° N, 19° N) representing mid- and low latitudes in China and found that the occurrence rate of Na sporadic layers were similar at locations less than 31° N but about 3 time smaller at 40° N. Na_s layers are common at low and high latitudes (Batista et al., 1989; Kwon et al., 1988; Hansen and von Zahn, 1990).

The occurrence of both sporadic-E and neutral layers has been linked to several processes that include neutralization, the presence of wind shears, and advection (Gardner et al., 1993; Tepley et al., 2003; Plane, 2004; Raizada et al., 2011,2012). Recently, Yuan et al. (2014) related the seasonal variations of Na_s and E_s layers to the convergence of metal ions in summer, while ion diffusion appeared to dominate in wintertime. Zhou et al. (2008) investigated the seasonal and local time variations of Fe_s and their relation to sporadic-E at Arecibo (18° N). They reported three nights of simultaneous observations of Fe and electron concentrations, where good correlations were seen in the occurrence of Fe_s with E_s layers. A correlative analysis between Na and Fe layers observed in China (30° N) revealed that the lower sides of these metal layers track each other extremely well, while the densities at the top side do not follow each other (Yi et al., 2008). They found that Na layer is broader and extends to higher altitudes; its upper boundary is about 5.2 km higher, while the lower boundary is ~0.6 km lower than Fe. Also, the temporal behavior of the upper boundary displayed some differences and was attributed to be likely due to sporadic layers. Recently, Yue et al. (2013) extended this study for the same metals observed at Arecibo with similar results showing that altitudinal dependence of Na and Fe correlations are global in nature. Both the studies did not compare the similarities or differences in sporadic activities, which is one of the goals in the current study.

Even though several studies of metal layers have been performed from different locations that have been mentioned in the above paragraphs, they were focused on other aspects of the metallic layers. In this study, we examine two cases of Na and Fe distributions along with simultaneous electron concentrations that were obtained using co-located resonance fluorescence lidars (RFLs) and incoherent scatter radar (ISR) at Arecibo (18.35° N, 66.75° W). The examples used in this investigation offer an excellent opportunity to improve our understanding related to metal layer response to sporadic-E and hence provide better insight about ion-neutral coupling. This study aims to understand the role played by various atmospheric constituents and other factors that may be responsible for differences observed in metallic layer.

Methods

The RFL system used for the measurements reported in this work consists of a single state of the art, Nd:YAG laser that pumps two identical dye lasers. The pumping was performed by splitting the second harmonic at 532 nm with 14 W of average power in each beam at 50-Hz repetition rate. The two dye lasers were tuned to generate resonance wavelengths of Na and Fe at 589 and 372 nm, respectively. We used the rhodamine 610 dye to generate the fundamental, 589-nm emission for Na, while the generation of the UV emission for 372 nm required a sum-frequency technique. So, for the second dye laser, we combined rhodamine 590 and 610 dyes for a dye fundamental at 572 nm and then sum frequency mixed with the IR residual from the Nd:YAG at 1064 nm to generate photons at 372 nm. The average power at this wavelength was ~1 W while at 589 nm, it was ~4 W. The backscattered photons were collected using an f/15 Cassegrain type telescope with a 0.8 m diameter. An optical fiber with a core diameter of 1.5 mm directed the light to a dichroic filter that splits the incoming beam to the detectors and narrow band interference filters of ~1-nm bandwidth at FWHM. EMI 9863-350B and Hamamatsu R943-02 photomultiplier tubes were used to collect the light at 372 and 589 nm, respectively. Other instrumental details can be found in the earlier work (Raizada and Tepley, 2002; 2003; Raizada et al., 2004; Tepley et al., 2003; Raizada et al., 2011; 2012).

The range resolution for all the lidar data presented here is 300 m. The temporal resolution for the Na and Fe datasets was ~1 min, and it was ~2 min for N_e.

The electron concentrations were derived from standard Barker-coded power profile measurements that were made during one of the topside ISR runs at Arecibo (González and Sulzer 1996). The technique utilizes a 13-baud, 4 μs/

baud coded pulse, yet we oversampled the data by a factor of 2 to yield a bin size of 300 m (Ioannidis and Farley 1972).

The background atmospheric conditions over Arecibo were monitored by using The Penn State Allsky Imager (PSASI), which records nighttime airglow at three different optical wavelengths (557.7, 630.0, 777.4 nm) that are emitted from different layers of the ionosphere. The 557.7-nm airglow comes from the upper mesosphere (~96 km) or E-region and its intensity is proportional to column-integrated $[O]^3$ (cube of concentration of atomic oxygen) in the emission layer. Since atomic oxygen is one of the major sources of ions and electrons in the lower E-region of the ionosphere, this emission can be used to monitor both neutral phenomena (such as gravity waves) and electrodynamics near this altitude. More details on PSASI, airglow, and ionospheric phenomena revealed by it can be found in Seker et al. (2007).

To obtain accurate information from the all-sky images, each image was processed in the following way. First, the images are spatially calibrated using star locations to find the geographic directions. Then, the stars are removed using a median filter and contrast is enhanced to better show the phenomena of interest (gravity waves). Finally, based on the location and coverage of the imager and height of the emission layer, the images are un-warped (to correct for the fish-eye lens effect) and then mapped to geographical coordinates.

Results

Co-located ISR and RFL measurements corresponding to the different metals offer an excellent way to understand mesospheric processes. Data pertaining to an alkali and a non-alkali meteoric metal measured at Arecibo on two consecutive nights, 17–18 and 18–19 March 2004, are discussed. These two cases represent sporadic-E events that are accompanied by a strong enhancement in the neutral Na but relatively weaker in Fe. We discuss these two nights in the following sections.

17–18 March 2004

Figure 1 displays the temporal and altitudinal distribution of electron, neutral Fe, and Na concentrations in the top, middle, and lower panels for 17 March 2004. The upper panel exhibits electron concentrations that are shown from 21:00 to 30 h LT (06:00 AST). This day was characterized by the presence of a very strong sporadic-E during the early part of the evening, with a descending layer from above 105 km that merges with a weak E_s at 97 km after 22:00 h AST. The false color scale in this figure has been saturated at values lower than maximum to provide a better contrast for weaker features. The maximum strength of the higher altitude E_s descending from 105 km at 18 h (AST) was $\sim 7 \times 10^4$ cm^{-3}, while the lower layer at 93 km

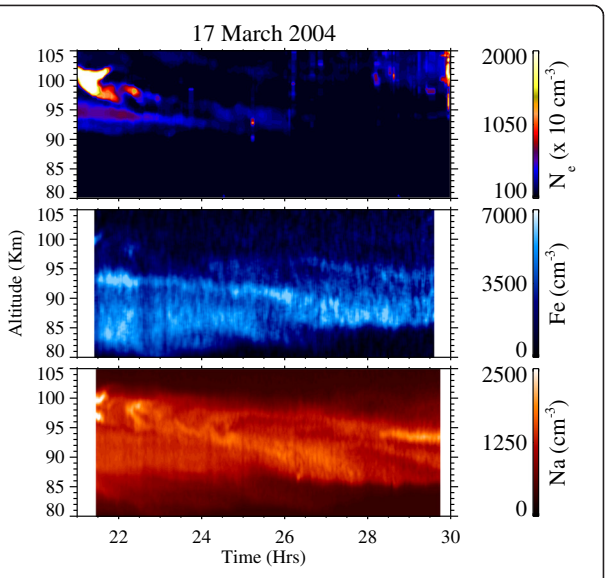

Fig. 1 Altitudinal and temporal variations of Ne (*upper panel*), neutral Fe (*middle panel*), and Na (*lower panel*) are shown for the night of 17–18 March 2004. Descending C-shaped structures (best seen in the Na distribution) are strong in both Ne and Na but weaker in the case of Fe

exhibited peak densities $\sim 1.9 \times 10^4$ cm^{-3}. The concentrations in both layers decreased by a factor of 7 and 4 in the upper and the lower regions, respectively, after 01:00 AST. The undulations observed in the electron distribution above 95 km are seen as "C" type structures, which are similar to those observed in Na distributions at another location (Clemesha, 2004). They appear to have periodicities varying between 0.5 and 1 h and descend at a rate of ~0.4 m/s. Such downward phase progressions have been attributed to tidal descending layers (Mathews and Bekeny, 1979; Mathews, 2001) and also observed earlier in the neutrals (Gardner et al., 1993, Raizada et al., 2012). The altitude-time-concentration plots of Fe and Na in the middle and the lower panel of Fig. 1 reveal bifurcated distributions of these metals with structures similar to the N_e distributions for both metals yet are stronger for Na than for Fe at altitudes exceeding 95 km. Such structures including billows have been observed in the Na distribution from Arecibo and other locations where these were attributed to wind shears and dynamical instabilities (Clemesha 2004; Sarkhel et al., 2012; Sarkhel et al., 2015a, b).

The quantitative relation between neutrals and plasma is further illustrated in Fig. 2. This figure displays the correlation coefficients (r) calculated for Na/N_e, Fe/N_e, and Na/Fe for two different altitude ranges that have been determined for a 5- or 4-km altitude interval that corresponds to about 25 or 20 data points at each time. In the upper altitude range (96–100 km), ion-neutral molecule chemistry dominates while the lower part (85–90 km) is governed by neutral chemistry. The upper panel displays the correlation between Na and N_e that is shown as a solid

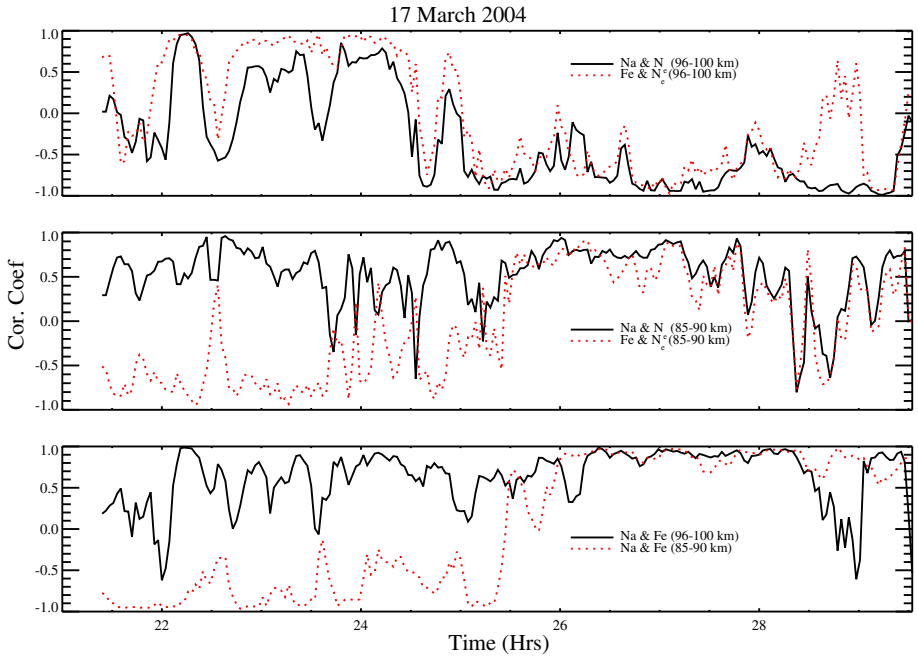

Fig. 2 This figure displays the temporal variation of correlation coefficient, *r*, in two altitude regions, one encompassing the upper part of the sporadic layer occurring between 96–100 km, while the other represents the 85–90-km region. The *top panel* displays *r* between Na and Ne (*solid line*) and Fe and Ne (*dashed line*) for the upper portion of the layer. The *middle panel* is similar to the above except for the 85–90-km region, while the *lower panel* represents *r* between neutrals only. The *solid/dashed lines* display the correlation between Na and Fe for the upper/lower part of the sporadic layers

line for 96–100 km, while the dashed line represents the temporal variation for Fe and N_e in the same altitude range. The neutralizations of both Na^+ and Fe^+ have negative temperature dependence, which can explain similar correlations of the neutrals with ions. Similarly, the middle panel shows the correlation coefficients calculated for the 85–90-km height interval. The lowest panel displays *r* determined only for the neutrals, i.e., Na and Fe, with solid/dashed lines showing upper/lower altitudes regions. However, between 85- and 90-km height intervals, both the neutrals behave similarly with Ne after 1:00 AM (LT) resulting in similar correlations with the latter. This is most likely due to the influence of neutral sporadic layer descending down to lower altitudes during the later part of the night. The early part of the night displays anti-correlation between Fe and Ne as compared to Na. This might be due to larger neutralization rates of Fe^+ to Fe as compared to Na, which will result in enhanced neutral densities in the case of former in presence of sporadic-E. This also explains anti-correlation between Na and Fe in 85–90-km region before midnight. The similar correlation between neutrals and N_e within the sporadic layer located at higher altitudes (96–100 km) indicates that Na and Fe are responding in a similar way to Ne. However, such correlation studies do not provide information regarding the strength of this neutral sporadic relative to the main layer.

The differences observed in the neutral sporadic activity are further elucidated in Fig. 3 that compares the strength of the Na and Fe distributions within a region centered at 97 ± 1.6 km relative to 87 ± 1.6 km. The higher altitude region largely coincides with the occurrence of sporadic-E, while the lower altitude region represents the main layer. To determine the intensity of the neutral sporadic event relative to the permanent or main layer, the average column concentrations in these two

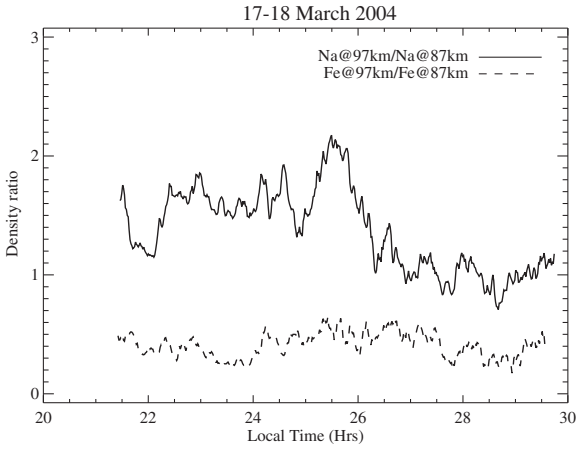

Fig. 3 This figure exhibits the ratio of concentration between the sporadic and the main layer for both Na (*solid line*) and Fe (*dashed line*). The ratio is determined by calculating the average densities in two regions of 3 km thickness centered around 97 and 87 km, representing the sporadic and main layers

altitude regions are calculated and their ratios are evaluated. The ratio of densities exceeding 1.0 indicates that the strength of the neutral layer at E_s altitudes is strong relative to the main layer. Figure 3 illustrates that the Na ratio at the two altitudes is greater than 1 before 26 h (02:00 AST) and decreased to lower values during the later part of the night as the layer descended. However, the neutral Fe behaves differently with ratios of less than 1.0 throughout the night. This shows quantitatively that the sporadic Fe (Fe_s) is less pronounced than Na_s.

Figure 4 exhibits the temporal variation of column abundance in the sporadic layers for Fe, Na, and N_e in the altitude range of 92–100 km. The left ordinate shows the neutral abundances while the N_e values are shown on the right axis. Both the neutral and electron concentrations reveal higher values associated with sporadic-E during the early part of the night, diminishing to lower values later. Larger values of Fe column abundances are consistent with the high content of this metal in chondrite meteoroids (Brown, 1973).

18–19 March 2004

Figure 5 displays the variation of electron concentrations, Fe and Na for the second night and is marked by E_s activity with electron concentrations $\sim 1.5 \times 10^4$ cm^{-3} occurring around 23 h (AST) centered at 95 km. However, this increase in N_e occurs suddenly and is not remnant of a strong descending layer during earlier times, which was the case for the previous night. The enhancement in N_e appears at 98 km and the layer moves down to 92 km, disappearing below this altitude level. This layer also bifurcates around 95 km into another layer that lasts for about 3 h more. Yet, the lack of a strong Fe_s corresponding to sporadic-E is noteworthy. Also, Fe concentrations in the main layer below 90 km are higher than those above 95 km, and this feature is consistent with the previous night. However, neutral sporadics are very well correlated with E_s activity in the upper altitude range of 96–100 km as depicted in Fig. 6, which is similar to Fig. 2. On this night, advection of a strong sporadic layer causes a correlation coefficient (r) to exceed 0.6 after 22:30 h (AST), as shown in the upper panel. The anti-correlations between neutrals and Ne before 22:30 h (LT) followed by positive r values have been observed in the case of other metals (Raizada et al., 2012). They attributed the positive correlations to the advection of the layers while the neutralization can lead to anti-correlation since decrease in Ne results in increase in the neutrals. The middle panel shows the temporal variation of correlation coefficients between N_e and Na (Fe) shown as solid (dashed) lines in the 85–90-km altitude region. This demonstrates that an increase in Na concentrations is associated with the increase in N_e, while an opposite trend is seen for Fe. Since on this night sporadic-E occurred above 90 km, the electron densities are not enough to cause appreciable neutralizations in the case of Fe. Their neutral concentrations would be determined by meteoric deposition balanced by the loss rate through the formation of stable compound like FeOH etc. in the lower part of the layer. Earlier studies by Zhou et al. (2008) have pointed out that a sporadic-E with electron concentrations exceeding 4000 electrons/cc can result in a strong Fe_s layer after sunset. In absence of any strong E_s activity below 95 km, Fe and Ne display anti-correlation. The third panel displays r between neutrals calculated for the upper layer (96–100 km, solid line) and the lower region (85–90 km, dashed line). It is observed that Na and Fe exhibit a very good correlation with values ~1.0 except for small durations that are separated by about 1–2-h time intervals in the upper altitude regions. In the 85–90-km region, the distribution of both neutrals is anti-correlated with each other between 23:00–24:00 h and will be discussed later. Figure 7, which shows the average density ratios of Na and Fe at two different altitude regions, corroborates that the sporadic neutral activity in the case of non-alkalis is weaker as compared to alkali metals. These ratios are found by taking the average densities at altitudes centered at 97 ± 1.6 and 87 ± 1.6 km, following the procedure that was used in Fig. 3. The results shown in this figure reveal that during strong E_s activity, Na concentrations at higher altitudes exceed the values at lower levels, making the density ratios greater than 1.0 during the event. However, the enhancement in sporadic Fe concentration did not exceed that in the main layer for this night, as was also the case of the previous night.

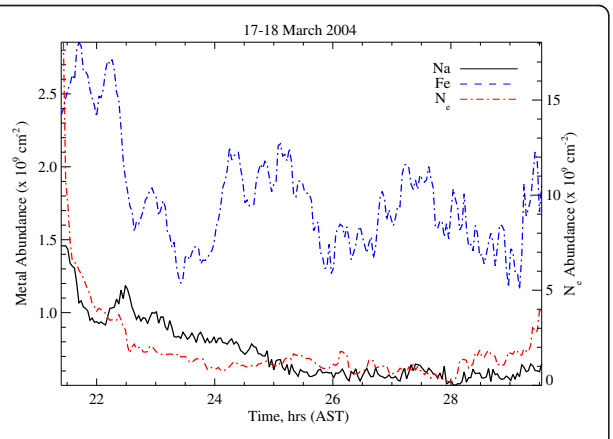

Fig. 4 This plot displays the temporal variation of column abundance of Ne (*dashed-dotted, red*), Fe (*dashed line, blue*), and Na (*solid line*). Note that the metal abundances are displayed on the left *Y*-axes while the *right ordinate* represents Ne values for the night of 17–18 March 2004 at Arecibo

The temporal variations of Na, Fe, (left ordinate) and N_e (right ordinate) column abundances determined from the Arecibo data for the night of 18 March 2004 are shown in Fig. 8. The observed primary peak in the N_e

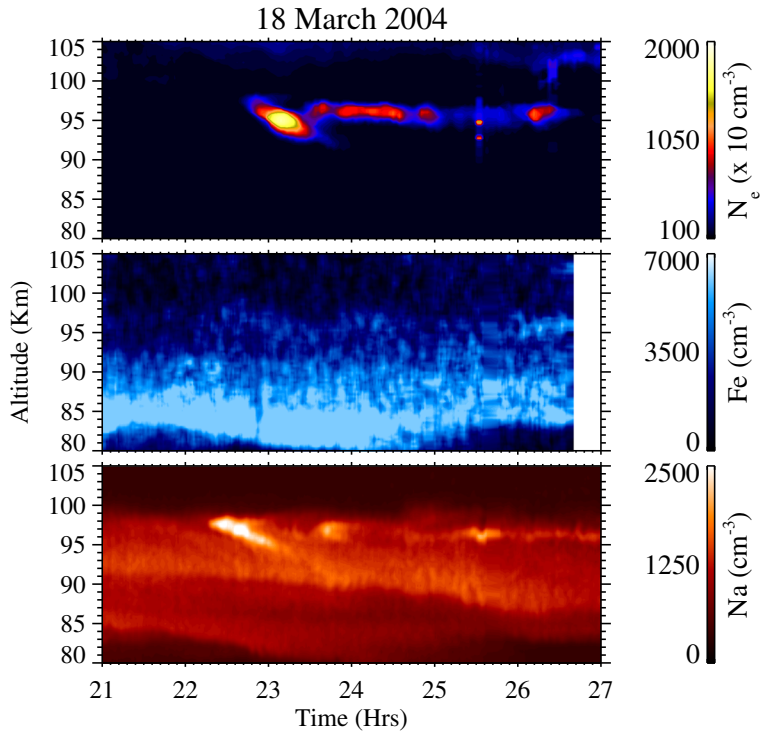

Fig. 5 This is similar to Fig. 1 but for the adjacent night. A good correspondence between neutral sporadic neutral and E_s layers is seen. However, Fe_s appears to be weaker than Na_s as compared to their main layers occurring below 90 km

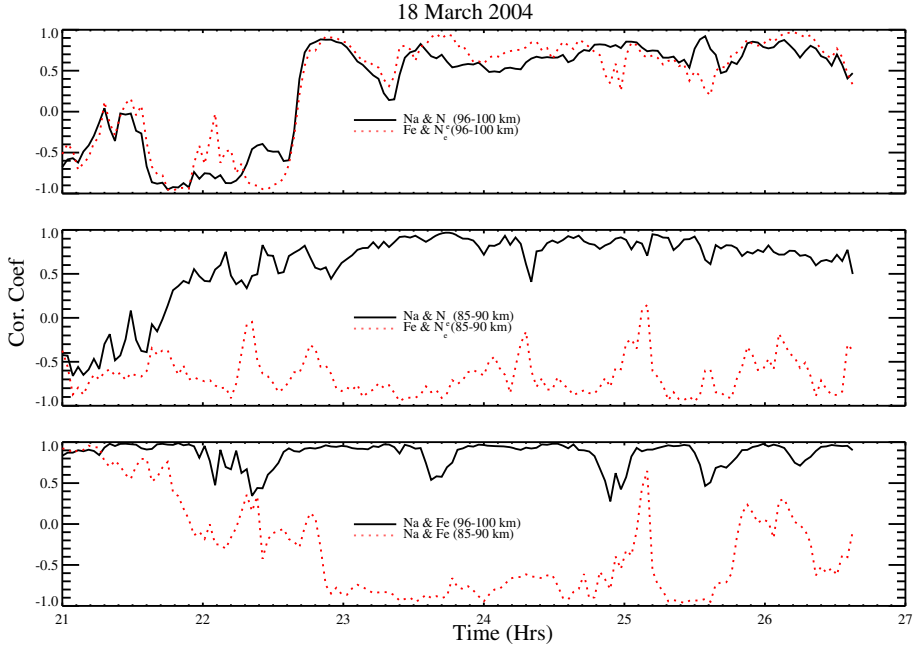

Fig. 6 This is similar to Fig. 2, except for the next night. Refer to the text for details

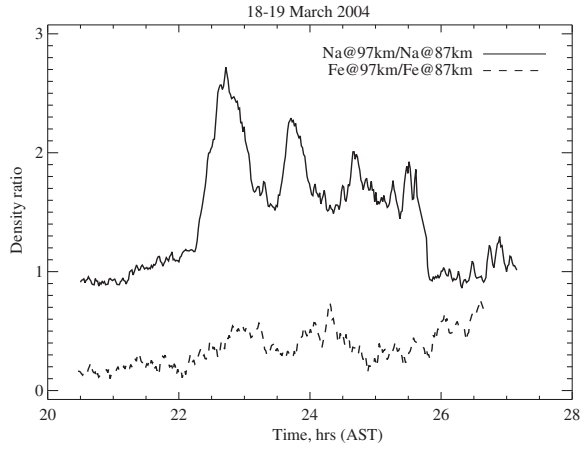

Fig. 7 This figure shows the temporal variation of density ratio for Na (*solid line*) and Fe (*dashed line*) at two altitude levels calculated in a similar way as in Fig. 3. The ratio exceeds 1 for the case of Na during the sporadic event and is less than 1 for Fe throughout the night of 18–19 March 2004

distribution coincides well with that seen in the Fe distribution around 23:20 h (AST). Also, the Na and N_e abundances display oscillations with a period of about an hour, as that observed in Fe. These aspects are discussed in the next section.

Additionally, to investigate the wave activity on these two nights, we further show the O(^{1}S) airglow images at 557.7 nm originating near 96-km altitude, obtained using the PSASI imager. Examples of images taken on 17–18 March and 18–19 March 2004 are shown in Fig. 9a, b. The detailed characteristics of the waves in the mesosphere on these nights are described in the "Discussion" section.

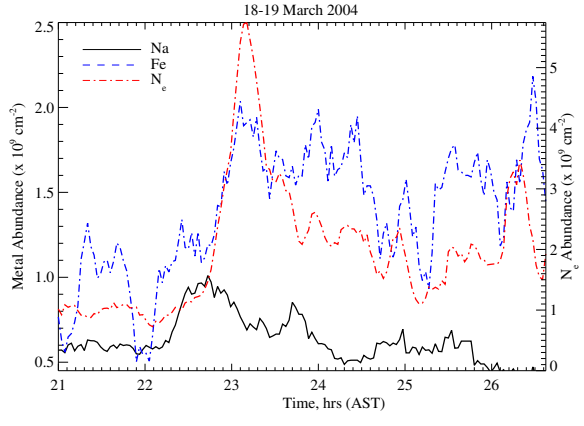

Fig. 8 This plot is similar to Fig. 4 except for the consecutive night. The Ne abundance (*dash-dot*, *red*) displays a peak at around 23:10 h (AST) that coincides with the Na concentration maximum (*solid line*, *left ordinate*)

Discussion

This work investigates two cases based on consecutive nights of lidar and ISR data obtained from Arecibo. Earlier studies have associated E_s layers with neutral distribution mainly through ion-molecule chemistry (Gardner et al., 1993; Collins et al., 2002; Raizada and Tepley, 2002; Zhou et al., 2008). The unique set of observations presented here illustrates the differences in neutral distribution and offers an excellent opportunity to understand the processes that can be responsible for such different behaviors observed for alkali and non-alkali metals. In this regard, it is important to compare the average/peak column abundances of Na and Fe in the main layer and also within E_s.

Table 1 lists the average and maximum column abundances of Na and Fe in the lower (82–92 km) and top (93–100 km) parts of the metal layers that were observed on the two nights reported herein, that is, 17–18 and 18–19 March 2004. Also given in the table are the N_e abundances in sporadic-E above 92 km only, since there were no substantial layers below this altitude. It is interesting to note that the peak N_e abundances were about 3 times higher on 17 March relative to the next night. However, the average abundances of N_e are similar on both nights, analogous to the average neutral abundances observed in the 93–100-km altitude region. It can be seen that Na abundance in the top part is about 1.4 times stronger than in the lower region, while for Fe an opposite behavior is observed with the upper layer about 1.2 times weaker than the latter on these nights. These abundances agree well with the earlier observations (Raizada and Tepley, 2003; Kane and Gardner, 1993; Zhou et al., 2005). Considering that both Fe and Fe^+ are dominant species in the nighttime mesosphere (Brown, 1973; Kopp 1997), a strong Fe_s activity compared to Na should be observed. Rocket measurements have revealed Fe^+ and Mg^+ to be the most abundant ions in the E-region (Kopp 1997). Ca^+ is the only ion that has been measured from ground-based lidars since all other metal ions have their resonance wavelengths in the UV part of the spectrum and are highly absorbed by ozone (Granier et al. 1989, Gardner et al., 1993; Gerding et al., 2000; Tepley et al., 2003; Raizada et al., 2011; 2012). The ratio of Ca^+/N_e concentrations and abundances inferred using in situ data obtained from Wallops Island rocket measurements is ~1–2 % and $\sim 4.27 \times 10^{-3}$, respectively (Kopp 1997). This agrees well with ground-based airglow and lidar measurements from Arecibo (Tepley et al., 1981, 2003; Raizada et al., 2012). Assuming that the fraction of Fe and Na ions in the E layer do not change drastically at Arecibo and Wallops, the fraction of these ions and abundances can be inferred using electron density information from ISR data. Thus, it is possible to estimate the Fe^+ and Na^+ abundances for the nights presented here by using

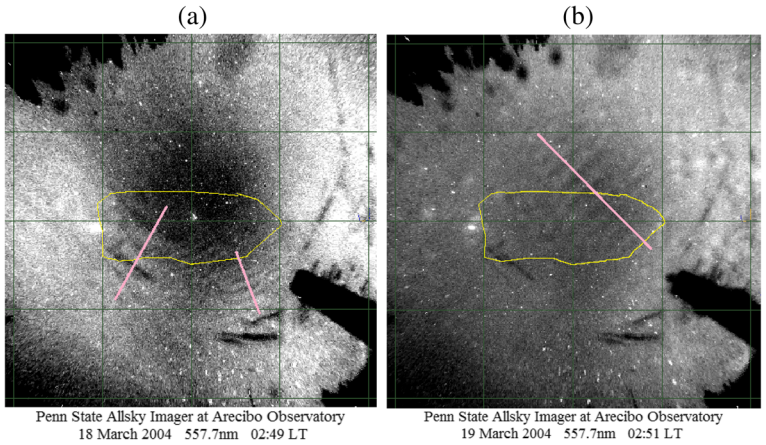

Fig. 9 All-sky images of the O(^{1}S) 557.7-nm airglow emission obtained using the PSU imager located at Arecibo: **a** a typical image taken on the night 17–18 March at 02:49 h (AST) showing wave activity with a *superimposed pink line* that indicates the phase progression; **b** an image representing data taken at 02:51 h (AST) for the consecutive night 18–19 March 2004

electron density profiles obtained using ISR data from Arecibo and prior in situ measurements of these ions. Table 2 compares the average abundances of Na^+ and Ca^+ normalized to Fe^+ that occur in carbonaceous chondrites with those obtained using rockets and estimated using ground-based electron concentrations from Arecibo. This table reveals that the average abundance of Fe ions over Arecibo is about 10 times larger than Na^+ within a sporadic-E layer during nighttime. However, a limitation of this technique arises from the fact that the in situ experiments were not performed from the same location or time as the ground-based experiments. Because Fe^+ has a much larger ion mass than the molecular ions [NO^+, O_2^+, N_2^+] or other metallic ions, it is possible that its concentration can be estimated by fitting the incoherent scatter spectra (Behnke and Vickrey, 1975; Tepley and Mathews, 1985). We hope to be able to verify the earlier conclusions regarding Fe^+ with future ISR experiments.

Earlier studies from Arecibo have shown a good correlation between sporadic-E and Fe_s layers (Raizada and Tepley, 2002; Zhou et al., 2008). The current study shows a good correlation between neutral sporadic and E_s layers in the altitude range of 96–100 km. The neutralizations of both Na^+ and Fe^+ have negative temperature dependence, which can explain such behavior. Between 85–90-km altitude intervals, the correlation between Na and Fe is similar when the sporadic-E descends to lower altitudes; otherwise these metals display different response to Ne. The simultaneous occurrence of sporadic neutral and E_s layers also results in good correlation between Na and Fe but results in poor correlation in absence of such coincidence. Yue et al. (2013) investigated altitudinal correlations between Na and Fe and found negative correlation coefficients (r) occurring in a narrow middle region encompassed by positive r values at the top and bottom parts of the layers. They demonstrated that the layer structure for the case of Na and Fe is mainly determined by chemistry, while the correlation between the two species is governed by gravity wave-induced density fluctuations. However, they determined r using the average data for all the night and to obtain its temporal variation, a sliding window of 1 h was used. Additionally, the work presented by Yue et al. (2013) did not study the influence of electron concentration on the neutrals due to the lack of ISR data. Since in this study, we aim at investigating the ion-neutral coupling, the correlations have been determined for specific altitude regions based on chemical differences. Later, we determine the chemical lifetimes of Fe and Na ions to shed more light on correlations.

The lidar gives the temporal variation of a particular metal along the line of sight and its altitudinal variation is often referred to as "lidargrams" (Clemesha et al., 2004).

Table 1 Average and peak abundances for Na, Fe, and N_e on two nights at Arecibo

Date	Altitude (km)	Na abundance ($10^9 \times cm^{-2}$)		Fe abundance ($10^9 \times cm^{-2}$)		Ne abundance ($10^9 \times cm^{-2}$)	
		Average	Max.	Average	Max.	Average	Max.
17 March 2004	82–92	0.5	0.9	4.2	5.5	-	-
	93–103	0.8	1.4	2.0	2.8	1.8	18.0
18 March 2004	82–92	0.7	0.9	5.4	6.8	-	-
	93–103	0.8	1.2	1.7	2.1	2.0	5.7

Table 2 Comparing the relative abundances of ions of chondrites in the MLT region

Relative abundance	Meteoroids	Rockets	ISR (Arecibo)
Fe^+	1	1	1
Na^+	6.3×10^{-2}	7.4×10^{-2}	9.1×10^{-2}
Ca^+	6.8×10^{-2}	2.8×10^{-2}	3.9×10^{-2}

Thus, both radar and lidar sample the line of sight volume of the atmosphere and do not provide any information regarding the spatial variability in horizontal dimensions. Collins et al. (2002) has discussed this aspect in detail. Earlier measurements have revealed structured sporadic-E with sizes ~300 m, limited by the range resolution of the radar (Miller and Smith, 1975). Later on, Hysell et al. (2012) found irregular sporadic-E with periodic structuring that was attributed to shear instability in the neutral flow. Though the medium can be inhomogeneous, the altitudinal/temporal resolution profiles at a given location can be useful to determine the variations, which can be caused either by dynamics or chemistry. A good correlation between metals is often observed apart from inhomogeneity in the atmosphere. The evidence comes from similarity between the lower boundary of Na and Fe layers as observed in the data presented in this study (Figs. 1 and 4), which is consistent with earlier observations (Yi et al., 2008; Yue et al. 2013). This suggests that local dynamics plays a significant role in the temporal variation of Na and Fe on any given night. The influence of E_s through ion-neutral coupling is evident from high correlations between the metals and Ne in the presence of sporadic-E. In the absence of strong Es, particularly between 85- and 90-km regions, Na and Fe display anti-correlation but changes to good correlation as the sporadic-E layers descend to lower altitudes (Fig. 2). This elucidates a different sensitivity of Na and Fe to electron concentrations. Also, the concentration ratios evaluated for both the neutral in the upper altitudes and within the main layer reveal that the latter is stronger in the case of Fe relative to its sporadic, which is an opposite behavior to the alkali metal, Na, on the two nights reported here. The possible reasons for this different sporadic activity in the neutral Fe and Na are discussed below.

Earlier studies have shown that the structure and distribution of different mesospheric metals are governed both by dynamics and chemistry (Plane, 2003; Gerding et al., 2000; Yue et al. 2013). To investigate the dynamical activity on these nights, we use the PSASI imager that reveals wave characteristics on these two nights. It is to be noted that imagers are well-suited instruments that provide information about gravity waves, MSTIDS (Makela et al., 2010). Figure 9a displays a GW event on the night of 17–18 March 2004 as measured from the O(^{1}S) 557.7-nm emission. This night is characterized by ripple-type (smaller wavelength, faster speed) and band-type (larger wavelength, slower speed) gravity waves (GWs) that were seen from 02:00 until 05:00 AST. Two separate GWs were observed around 03:00 AST. The first GW packet appeared southwest of the Arecibo and was aligned along the northwest-southeast direction and moved slightly westward of the north direction, disappearing toward the northwest of Arecibo. The horizontal wavelength, speed, and period of the GWs were measured as ~25 km, 2.5 km/min (150 km/h or ~40 m/s), and 10 min, respectively. These values are typical for E-region band-type (large-scale, slow speed) GWs. The second GW packet appeared southeast of Arecibo and propagated northward. The horizontal wavelength, speed, and period of the GWs were measured as ~10 km, 1.5 km/min (90 km/h or 25 m/s), and ~7 min, respectively. This wavelength value is typical for E-region ripple-type GWs (Chung et al., 2003).

Figure 9b shows the wave activity, again observed at 557.7 nm, obtained on the night of 18–19 March 2004. This night is also characterized by both band-type and ripple-type GWs. Ripple-type GWs were dominant, especially during 02:30–03:30 h AST and all-sky band-type GWs were dominant during 04:00 h AST. The ripple-type GWs appeared northeast of Arecibo, were aligned along northeast-southwest, and moved toward the northwest, disappearing north of the site. The horizontal wavelength, speed, and period of the GWs were measured as ~20 km, 2.5 km/min (150 km/h or ~40 m/s), and 8 min, respectively. The band-type GWs covered the whole sky, were aligned northwest-southeast, and propagated southwestward. The horizontal wavelength, speed, and period of the band-type GWs were measured as ~14 km, 1 km/min (60 km/h or ~17 m/s), and 14 min, respectively.

Thus, the PSASI imager data reveal that both nights had similar wave structure, which can also cause temperature perturbations. The occurrence of ripple-type structures seen on both the nights suggests that the atmospheric conditions are conducive for dynamical instabilities, which are likely to occur in the presence of strong horizontal shears. As discussed in the above paragraph, the ripple-type structures appear to propagate in meridional direction with a component in the zonal direction. This implies the possibility of existence of large horizontal wind shears that are required for E_s formation (Whitehead, 1989). This is consistent with the ISR observations of sporadic-E layer on both the nights. Recent studies by Fytterer et al. (2014) revealed that the amplitude of 8-h E_s maximizes during equinox at low and mid-latitudes in both hemispheres.

Previous studies have shown that the variability in mesospheric temperatures during sporadic events is ~30 K over Arecibo (Friedman et al., 2003). Climatological studies have revealed that tides resulted in a 20-K

variation in mesospheric temperature in March over Arecibo (Friedman and Chu, 2007). Such temperature fluctuations can influence the mesospheric chemistry, which can affect the strength of sporadic neutral layers as a result of ion-neutral coupling. The Na dayglow intensity variations observed for a few days from Trivandrum (India), a low-latitude station, have been attributed to chemistry (Hossain et al., 2014). Another factor mentioned previously that can affect the strength of neutral sporadic activity can be due to inhomogeneity in the medium or advection, but that alone cannot explain why the minor species like Na show stronger sporadic layer as compared to one of the major metals like Fe relative to their main or permanent layers. Thus, to gain better insight, we compare the lifetimes of Na and Fe ions against neutralization based on previous studies (Cox and Plane, 1997; Helmer et al., 1998; Collins et al., 2002; Woodcock et al., 2006). Collins et al. (2002) have shown that Na^+ neutralization decreases sharply below 100 km as compared to Fe^+. At altitudes around 95 km, ion-molecule chemistry dominates, with the Na layer being influenced by the formation of ligands like $Na^+.CO_2$, $Na^+.N_2$. These cluster ions undergo dissociative recombination with electrons resulting in their neutralization. However, $Na^+.N_2$ can react with atomic O to form NaO^+, which can result in Na^+ formation through its reaction with another atomic O. Thus, the overall rate of neutralization is controlled by the altitude-dependent ratio of $[CO_2]$:[O], which increases below 100 km. In the case of Fe^+, Vondrak et al. (2006) have shown the importance of $Fe^+.N_2$, $Fe^+.O_2$, and FeO^+ ions in governing their chemical lifetimes through dissociative recombination with electrons. Since formation of $Fe^+.N_2$, $Fe^+.O_2$ involves a third body (i.e., they are termolecular reaction), their rates increase below 85 km while FeO^+ dominates above this altitude. We calculate the neutralization lifetimes of Na^+ and Fe^+ based on the chemistry discussed in Collins et al. (2002) and Vondrak et al. (2006), respectively. The reactions rates have been taken from their work, while the MSIS-90 model has been used to infer neutral densities like O_2 and N_2. Minor species like CO_2 and H_2O are taken from Swider (1996), while O_3 profiles are obtained using the CIRA 1986 model. Figure 10 displays the altitude variation of lifetimes of Fe^+ and Na^+ against neutralization. This figure reveals that Fe ions have a longer lifetime compared with Na^+, which will result in a more rapid neutralization of the latter resulting in stronger neutral Na sporadic layers compared with the former. Also shown is the sensitivity of these ions to neutral temperature and to minor species. Both Na^+ and Fe^+ are sensitive to temperature changes but have different altitudinal dependence. Na ion lifetimes exhibit a ±23–24 % variation for a ±10 % change in temperature, which does not change with altitude. Such temperature change produces a variable response in Fe^+ lifetimes (~23–1 %), i.e., larger at lower altitudes as compared to higher altitudes. Thus, temperature-induced variability in Fe^+ lifetimes is going to be greater than 10 % below 100 km and decreases above this altitude. Plane et al. (1999) showed that since Na^+ chemistry involves ligand formations, which have square

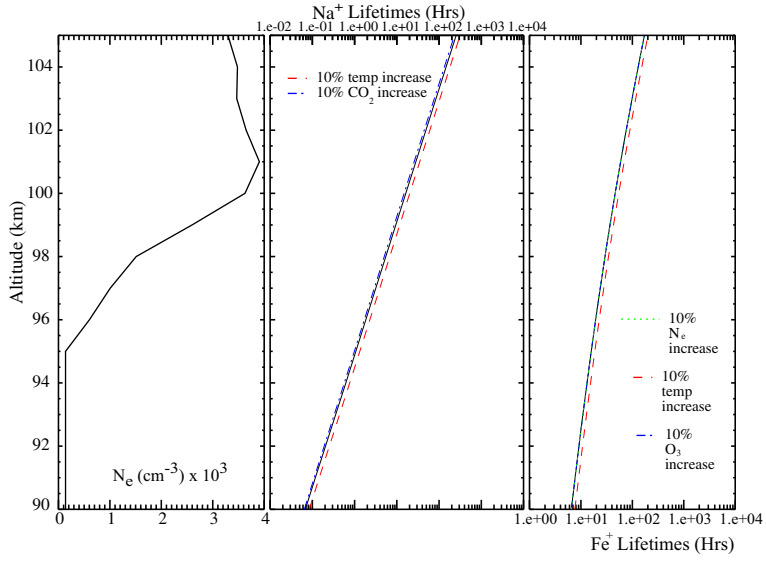

Fig. 10 The *left panel* shows the altitude variation of electron density that represents a typical variation of the sporadic-E layer for the nights shown in this work. The *middle panel* displays the lifetimes of Na ions against neutralization (*solid line*) with *superimposed dashed lines* showing the change in the lifetime due to a ±10 % increase in the temperature. Also displayed is the *dashed-dotted line* showing the change due to a 10 % increase in CO_2 concentration. The *right panel* exhibits Fe^+ chemical lifetimes (*solid line*). The superimposed lines (*thick dashed*, *dashed-dotted*, *thin-dashed*) display the new lifetimes due to 10 % changes in temperature, ozone, and Ne values, respectively

dependence on atmospheric density, they are more sensitive to its change as compared to Fe ions. The latter also displays more sensitivity to Ne changes relative to Na ions. A ±10 % change in N_e concentrations results in negligible variations in the latter, while it causes about 9–10 % changes in the former metal. This is consistent with the earlier work by Zhou et al. (2008) showed a dependence of strong Fe_s activity on Ne exceeding 4000 electrons cm^{-3}. On the nights reported here, a weak Fe_s was observed corresponding to sporadic-E with electron less than 4000 electrons cm^{-3}. Similarly, increasing CO_2 by 10 % causes a ~9 % decrease in Na^+ lifetimes, while an increase of 10 % in ozone has negligible influence on Fe^+ lifetimes at all altitudes. The changes in the concentrations of minor species can occur due to advection or horizontal transport, however that will cause minor variability in the neutralization lifetimes of Na and Fe ions. But these are more sensitive to temperature variations that can result from GWs, dynamical instabilities, ripple-type structures that were observed on these nights. Hence, any fluctuation in this parameter will influence the neutralization process. Earlier studies have found the Na abundance to be sensitive to temperature changes (Zhou et al., 1993). Temperature perturbations can result in compressional or dissipative heating depending on the ambient conditions.

The differences in lifetime sensitivity to electron concentrations manifest in correlation seen in the Figs. 2 and 6. The anti-correlation between Na and Fe in the lower part (85–90 km) on both the nights can possibly be attributed to longer Fe^+ lifetimes and higher sensitivity to Ne concentrations relative to Na.

This work suggests that the stronger Na sporadic layer can result from the faster neutralization process, which is more sensitive to temperature changes compared with Fe at altitudes above 100 km. Our data suggests that the stronger structures in the case of Na compared with Fe within sporadic neutral layer are more likely to be the manifestation of temperature-induced lifetime variability. Thus, it appears that Na acts as better tracer for studying gravity wave-induced fluctuations at higher altitudes.

Conclusions

Two adjacent nights of simultaneous Na, Fe, and N_e data from Arecibo were studied to examine their characteristics. Fe^+, being one of the most abundant ions in the upper mesosphere, makes its neutral species counterpart an interesting element to be studied, in particular when electron concentrations and measurements of other metals are available. An estimation of the concentration of ions within sporadic-E events observed at Arecibo during nighttime reveals that the Fe^+ and Na^+ concentrations are ~600 and 30 ions.cm^{-3}, respectively. The strength of the neutral sporadic layers is determined by evaluating the ratios of the concentrations above 90 km to that of the main layer. This value is larger for Na compared with Fe, indicating that sporadic activity in Na is stronger than the more abundant metal, Fe on the two nights reported here. Thus, this suggests that each metal responds differently to E_s layers. Several factors like dynamics and chemistry can contribute to the differences in sporadic activity. Airglow images obtained at 557.7 nm indicate similar dynamical activity on the two nights with ripple-type structures suggesting the occurrence of dynamical instabilities. This indicates the presence of large shears in the horizontal winds that are required for E_s formation. The sporadic-E activity observed in the ISR data supports this scenario. Inhomogeneity alone cannot account for a weaker sporadic Fe layer relative to its main layer, as this is one of the dominant species in the mesosphere. A comparison of lifetimes of these two metals reveals a faster neutralization for the alkali metal (Na), which is more sensitive to temperature changes than for changes in minor species concentrations. To summarize, the weaker, or less pronounced, sporadic events in Fe are most likely due to slower neutralization rates along with their lesser sensitivity to temperature changes.

Future work should focus on understanding the climatological distribution of simultaneous measurements of Na and Fe. Such studies will facilitate the appreciation of the role of dynamics and chemistry that can influence the structure of the metals layers and contribute to their seasonal as well as latitudinal and altitudinal variability.

Competing interests

The authors declare that they have no competing interests.

Authors' contributions

SR and CT carried out the lidar observations. SR perceived the idea and performed the calculations mentioned in this work. JDM and IS provided the imager data and were involved in analysis pertaining to imager data. NA and EC provided electron density data. QZ, CT, SS, IS, RK, JDM, NA, and EC assisted in the manuscript writing and provided their feedback to improve the quality of the work. All authors read and approved the final manuscript.

Acknowledgements

We acknowledge the National Science Foundation (NSF) grants AGS-1243063, AGS-1241436 to SRI International, USA and AGS-1243133 to Miami University, USA that allowed us to carry out the research for this paper. J. D. Mathews' and part of S. Sarkhel's component were supported by a NSF grant AGS 1241407 to The Pennsylvania State University, USA. S. Raizada is extremely grateful to Raúl García for providing technical support. The Arecibo Observatory is operated by SRI International under a cooperative agreement with the National Science Foundation (AST-1100968) and in alliance with Ana G. Méndez—Universidad Metropolitana and the Universities Space Research Association.

Author details

[1]Space and Atmospheric Sciences, Arecibo Observatory, SRI International, Arecibo, PR, USA. [2]Electrical and Computer Engineering Department, Miami University, Oxford, OH, USA. [3]Department of Physics, Indian Institute of Technology Roorkee, Roorkee 247667, Uttarakhand, India. [4]Radar Space Sciences Laboratory, The Pennsylvania State University, 323 Electrical Engineering East, University Park, PA, USA. [5]Radar Systems Engineering Department Radar, Intelligence ASELSAN Inc, Ankara, Turkey.

Received: 2 March 2015 Accepted: 2 September 2015
Published online: 11 September 2015

References

Alpers M, Höffner J, von Zahn U (1990) Iron atom densities in the polar mesosphere from lidar observations. Geophys Res Lett 17:2345–2346
Alpers M, Höffner J, von Zahn U (1994) Sporadic Fe and E layers at polar, middle, and low latitudes. J Geophys Res 99:14,971–14,985
Batista PP, Cieraesha BR, Batism IS, Simonich C DM (1989) Characteristics of the sporadic sodium layers observed at 23° S. J Geophys Res 94:15,349–15,358
Behnke RA, Vickrey JF (1975) Radar evidence for Fe^+ in a sporadic-E layer. Radio Sci l0:325–327
Brown TL (1973) The chemistry of metallic elements in the ionosphere and mesosphere. Chem Rev 73(6):645–667
Chu X, Espy PJ, Knott GJ, Diettrich JC, Gardner CS (2006) Polar mesospheric clouds observed by an iron Boltzmann lidar at Rothera (67.5° S, 68.0° W), Antarctica from 2002 to 2005: properties and implications. J Geophys Res 111:D20213. doi:10.1029/2006JD007086
Chung J-K, Kim YH, Won Y-I (2003) Observation of mesospheric waves with an all-sky camera in Korean Peninsula. Adv Space Res 32(5):825–830. doi:10.1016/S0273-1177(03)00414-9
Clemesha BR (2004) A review of recent MLT studies at low latitudes. Ann Geophys 22:3261–3275. doi:10.5194/angeo-22-3261-2004
Clemesha BR, Batista PP, Simonich DM, Batista IS (2004) Sporadic structures in the atmospheric sodium layer. J Geophys Res 109:D11306. doi:10.1029/2003JD004496
Collins RL, Nomura A, Gardner CS (1994) Gravity waves in the upper mesosphere over Antarctica: lidar observations at the South Pole and Syowa. J Geophys Res 99:5475–5485. doi:10.1029/93JD03276
Collins SC, Plane JMC, Kelley MC, Wright TG, Soldan P, Kane TJ, Gerrard AJ, Grime BW, Rollason RJ, Friedman JS, Gonzalez SA, Zhou Q, Sulzer MP, Tepley CA (2002) A study of the role of ion–molecule chemistry in the formation of sporadic sodium layers. J Atmos Terr Phys 64:845–860
Cox RM, Plane JMC (1997) An experimental and theoretical study of the clustering reactions between Na^+ ions and N_2, O_2 and CO_2. J Chem Soc Faraday Trans 93:2619–2629
Friedman JS, Tepley CA, Raizada S, Zhou QH, Hedin J, Delgado R (2003) Potassium Doppler-resonance lidar for the study of the mesosphere and lower thermosphere at the Arecibo Observatory. J Atmos Sol Terr Phys 65:1411–1424. doi:10.1016/j.jastp.2003.09.004
Dou XK, Qiu SC, Xue XH, Chen TD, Ning BQ (2013) Sporadic and thermospheric enhanced sodium layers observed by a lidar chain over China. J Geophys Res Space Phys 118:6627–6643. doi:10.1002/jgra.50579
Friedman JS, Chu X (2007) Nocturnal temperature structure in the mesopause region over the Arecibo Observatory (18.35° N, 66.75° W): seasonal variations. J Geophys Res 112:D14107. doi:10.1029/2006JD008220
Fytterer T, Arras C, Hoffmann P, Jacobi C (2014) Global distribution of the migrating terdiurnal tide seen in sporadic E occurrence frequencies obtained from GPS radio occultations. Earth Planets Space. doi:10.1186/1880-5981-66-79.
Gadsden M (1969) Antarctic twilight observations, 1, search for metallic emission lines. Ann Geophys 25:667–677
Gardner CS, Kane TJ, Senft DC, Qian J, Papen GC (1993) Simultaneous observations of sporadic E, Na, Fe, and Ca^+ layers at Urbana, Illinois: three case studies. J Geophys Res 98(D9):16,865–16,873
Gardner CS, Chu X, Espy PJ, Plane JMC, Marsh DR, Janches D (2011) Seasonal variations of the mesospheric Fe layer at Rothera, Antarctica (67.5° S, 68.0° W). J Geophys Res 116:D02304. doi:10.1029/2010JD014655
Granier C, Jegou JP, Megie G (1989) Iron atoms and metallic species in the Earth's upper atmosphere. Geophys Res Lett 16:243–246
Gerding M, Alpers M, von Zahn U, Rollason RJ, Plane JMC (2000) The atmospheric Ca and Ca^+ layers: mid-latitude observations and modeling. J Geophys Res 105:27131–27146
González SA, Sulzer MP (1996) Detection of He^+ layering in the topside ionosphere over Arecibo during equinox solar minimum conditions. Geophys Res Lett 23:2,509–2,512
Hansen G, von Zahn U (1990) Sudden sodium layers in polar latitudes. J Atmos Terr Phys 52:585–608
Helmer M, Plane JMC, Qian J, Gardner CS (1998) A model of meteoric iron in the upper atmosphere. J Geophys Res 103:10913
Md Mosarraf Hossain, Vineeth C N, Nair S, Sumod G K, Pant T K (2014) Highly varying daytime sodium airglow emissions over an equatorial station: a case study based on the measurements using a grating monochromator. Earth Planets Space. doi:10.1186/1880-5981-66-56.
Huang W, Chu X, Gardner CS, Wang Z, Fong W, Smith JA, Roberts BR (2013) Simultaneous, common-volume lidar observations and theoretical studies of correlations among Fe/Na layers and temperatures in the mesosphere and lower thermosphere at boulder table mountain (40° N, 105° W), Colorado. J Geophys Res 118:8748–8759. doi:10.1002/jgrd.50670
Hysell DL, Nossa E, Larsen MF, Munro J, Smith S, Sulzer MP, González SA (2012) Dynamic instability in the lower thermosphere inferred from irregular sporadic E layers. J Geophys Res 117:A08305. doi:10.1029/2012JA017910
Ioannidis G, Farley DT (1972) Incoherent scatter observations at Arecibo using compressed pulses. Geophys Res Letts 7(7):763–766
Kane TJ, Gardner CS (1993) Structure and seasonal variability of the nighttime mesospheric Fe layer at midlatitudes. J Geophys Res 98:16,875–16,886
Kirkwood S, von Zahn U (1991) On the role of auroral electric fields in the formation of low altitude sporadic-E and sudden sodium layers. J Atmos Terr Phys 53:389–407
Kopp E (1997) On the abundance of metal ions in the lower ionosphere. J Geophys Res 102:9667–9674
Kwon KH, Senft DC, Gardner CS (1988) Lidar observations of sporadic sodium layers at Mauna Kea Observatory, Hawaii. J Geophys Res 93(14):199–14,208
Makela JJ, Miller ES, Talaat ER (2010) Nighttime medium-scale traveling ionospheric disturbances at low geomagnetic latitudes. Geophys Res Lett 37(L24):104. doi:10.1029/2010GL045922
Mathews JD, Bekeny FS (1979) Upper atmosphere tides and the vertical motion of ionospheric sporadic layers at Arecibo. J Geophys Res 84:2743–2750
Mathews JD, Machuga DW, Zhou Q (2001) Evidence for electrodynamic linkages between spread-F, ion rain, the intermediate layer, and sporadic E: results from observations and simulations. JASTP 63:1529–1543
Miller KL, Smith LG (1975) Horizontal structure of midlatitude sporadic-E layers observed by incoherent scatter radar. Radio Sci 10(3):271–276
Nagasawa C, Abo M (1995) Lidar observations of a lot of sporadic sodium layers in mid-latitude. Geophys Res Letts 22(3):263–266
Plane JMC, Cox RM, Rollason RJ (1999) Metallic layers in the mesopause and lower thermosphere region. Adv Space Res 24:1559–1570
Plane JMC (2003) Atmospheric chemistry of meteoric metals. Chem Rev 103:4963–4984
Plane JMC (2004) A time-resolved model of the mesospheric Na layer: constraints on the meteor input function. Atmos Chem Phys Discuss 4:39–69
Raizada S, Tepley CA (2002) Iron Boltzmann lidar temperature and density observations from Arecibo—an initial comparison with other techniques. Geophys Res Lett 29(12):1560
Raizada S, Tepley CA (2003) Seasonal variation of mesospheric iron layers at Arecibo: first results from low-latitudes. Geophys Res Lett 30:1082
Raizada S, Tepley CA, Janches D, Friedman JS, Zhou Q, Mathews JD (2004) Lidar observations of Ca and K metallic layers from Arecibo and comparison with micrometeor sporadic activity. J Atmos Sol Terr Phys 66:595–606
Raizada S, Tepley CA, Aponte N, Cabassa E (2011) Characteristics of neutral calcium and Ca^+ near the mesopause, and their relationship with sporadic ion/electron layers at Arecibo. Geophys Res Lett 38:L09103. doi:10.1029/2011GL047327
Raizada S, Tepley CA, Williams BP, Garcia R (2012) Summer to winter variability in mesospheric calcium ion distribution and its dependence on Sporadic E at Arecibo. J Geophys Res 117:A02303. doi:10.1029/2011JA01695
Rapp M, Lübken F-J (2004) Polar mesosphere summer echoes (PMSE): review of observations and current understanding. Atmos Chem Phys 4:2601–2633
Sarkhel S, Raizada S, Mathews JD, Smith S, Tepley CA, Rivera F, Gonzalez SA (2012) Identification of large scale billows-like structure in the neutral Na layer over Arecibo. J Geophys Res 117:A10301. doi:10.1029/2012JA017891
Sarkhel S, Mathews JD, Shikha R, Sekar R, Chakrabarty D, Guharay A, Jee G, Kim J-H, Kerr RB, Geetha R, Sridharan S, Wu Q, Mlynczak MG, Russell JM, III (2015) A case study on occurrence of an unusual structure in the sodium layer over Gadanki, India. Earth Planets Space 67:19. doi:10.1186/s40623-015-0183-5
Sarkhel S, Mathews JD, Shikha R, Ramanathan S, Dibyendu C, Amitava G, Geonhwa J, Jeong-Han K, Kerr RB, Geetha R, Sundararajan S, Qian W, Mlynczak MG, Russell JM (2015b) Erratum to: A case study on occurrence of an unusual structure in the sodium layer over Gadanki, India. Earth Planets Space 67:145. doi:10.1186/s40623-015-0276-1
Seker I, Mathews JD, Wiig J, Guiterrez PF, Friedman JS, Tepley CA (2007) First results from the Penn State all sky imager at the Arecibo Observatory. Earth Planets Space 59:165–176
Sridharan S, Vishnu Prasanth P, BhavaniKumar Y, Geetha R, Sathishkumar S, Raghunath K (2009) Observations of peculiar sporadic sodium structures and their relation with wind variations. J Atmos Sol Terr Phys 71:575–582

Swider W (1996) Steady state D-region model, published in the book: Solar-Terrestrial Energy Proram (STEP). In: Schunk RW (ed) Handbook of ionospheric models

Tepley CA, Mathews JD (1985) An incoherent scatter radar measurement of the average ion mass and temperature of a nighttime sporadic layer. J Geophys Res 90:3517–3519

Tepley CA, Mathews JD, Meriwether JW, Walker JCG (1981) Observations of the Ca^+ twilight airglow from intermediate layers of ionization. J Geophys Res 86:7781–7786

Tepley CA et al (2003) First simultaneous observations of Ca^+, K, and electron density using lidar and incoherent scatter radar at Arecibo. Geophys Res Lett 30(1):1009. doi:10.1029/2002GL015927

Vondrak T, Woodcock KRS, Plane JMC (2006) Phys Chem Chem Phys 8:503

Wang J, Yang Y, Cheng X, Yang G, Song S, Gong S (2012) Double sodium layers observation over Beijing, China. Geophys Res Lett 39:L15801. doi:10.1029/2012GL052134

Whitehead JD (1989) Recent work on mid-latitude and equatorial Sporadic-E. J Atmos Terr Phys 51(5):401–424

Williams BP, Berkey FT, Sherman J, She C-Y (2007) Coincident extremely large sporadic sodium and sporadic E layers observed in the lower thermosphere over Colorado and Utah. Ann Geophys 25:3–8

Woodcock KR, Vondrak ST, Meech SR, Planew JMC (2006) A kinetic study of the reactions $FeO^+ + O$, $Fe^+ N_2 + O$, $Fe^{+\cdot} O_2 + O$ and $FeO^+ + CO$: implications for sporadic E layers in the upper atmosphere. Phys Chem Chem Phys 8:1812–1821. doi:10.1039/b518155k

Yi F, Zhang SD, Zeng HJ, He YJ, Yue XC, Liu JB, H FL, Xiong DH (2002) Lidar observations of sporadic Na layers over Wuhan (30.5° N, 114.4° N). Geophys Res Lett 29(9):1345. doi:10.1029/2001GL014353

Yi F, Zhang S, Yue X, He Y, Yu C, Huang C, Li W (2008) Some ubiquitous features of the mesospheric Fe and Na layer borders from simultaneous and common-volume Fe and Na lidar observations. J Geophys Res 113:A04S91. doi:10.1029/2007JA012632

Yuan T, Wang J, Xuguang C, Sojka J, Rice D, Oberheide J, Criddle N (2014) Investigation of the seasonal and local time variations of the high-altitude sporadic Na layer (Nas) formation and the associated midlatitude descending E layer (Es) in lower E region. JGR. doi:10.1002/2014JA019942

Yuan T, She C-Y, Kawahara TD, Krueger DA (2012) Seasonal variations of midlatitude mesospheric Na layer and their tidal period perturbations based on full diurnal cycle Na lidar observations of 2002–2008. J Geophys Res 117:D11304. doi:10.1029/2011JD017031

Yue X, Zhou Q, Raizada S, Tepley CA, Friedman JF (2013) Relationship between mesospheric Na and Fe layers from simultaneous and common-volume lidar observations at Arecibo. J Geophys Res. doi: 10.1002/jgrd.50148.

Zhou Q, Mathews JD, Tepley CA (1993) A proposed temperature dependent mechanism for the formation of sporadic sodium layers. J Atmos Sol Terr Phys 55(3):513–521

Zhou Q, Friedman J, Raizada S, Tepley CA, Morton YT (2005) Morphology of nighttime ion, potassium and sodium layers in the meteor zone above Arecibo. J Atmos Sol Terr Phys 67:1245–1257

Zhou Q, Raizada S, Tepley CA, Plane JMC (2008) Seasonal and diurnal variation of electron and iron concentrations at the meteor heights above Arecibo. J Atmos Sol Terr Phys 70:49–60. doi:10.1016/j.jastp.2007.09.012